

UC Irvine

UC Irvine Previously Published Works

Title

A Comparative Study of Vertebrate Corneal Structure: The Evolution of a Refractive Lens
Vertebrate Corneal Structure

Permalink

<https://escholarship.org/uc/item/5322242k>

Journal

Investigative Ophthalmology & Visual Science, 56(4)

ISSN

0146-0404

Authors

Winkler, Moritz
Shoa, Golroxan
Tran, Stephanie T
[et al.](#)

Publication Date

2015-04-30

DOI

10.1167/iovs.15-16584

Peer reviewed

A Comparative Study of Vertebrate Corneal Structure: The Evolution of a Refractive Lens

Moritz Winkler,¹ Golroxan Shoa,² Stephanie T. Tran,² Yilu Xie,² Sarah Thomasy,³ Vijay K. Raghunathan,³ Christopher Murphy,³ Donald J. Brown,^{1,2} and James V. Jester^{1,2}

¹Department of Biomedical Engineering, University of California-Irvine, Irvine, California, United States

²Gavin Herbert Eye Institute, University of California-Irvine, Irvine, California, United States

³University of California-Davis, Davis, California, United States

Correspondence: James V. Jester, 843 Health Sciences Road, Hewitt Hall, Room 2036, University of California, Irvine, Irvine, CA 92697-4390, USA; jjester@uci.edu.

Submitted: January 30, 2015

Accepted: March 23, 2015

Citation: Winkler M, Shoa G, Tran ST, et al. A comparative study of vertebrate corneal structure: the evolution of a refractive lens. *Invest Ophthalmol Vis Sci.* 2015;56:2764-2772. DOI:10.1167/iovs.15-16584

PURPOSE. Although corneal curvature plays an important role in determining the refractive power of the vertebrate eye, the mechanisms controlling corneal shape remain largely unknown. To address this question, we performed a comparative study of vertebrate corneal structure to identify potential evolutionarily based changes that correlate with the development of a corneal refractive lens.

METHODS. Nonlinear optical (NLO) imaging of second-harmonic-generated (SHG) signals was used to image collagen and three-dimensionally reconstruct the lamellar organization in corneas from different vertebrate clades.

RESULTS. Second-harmonic-generated images taken normal to the corneal surface showed that corneal collagen in all nonmammalian vertebrates was organized into sheets (fish and amphibians) or ribbons (reptiles and birds) extending from limbus to limbus that were oriented nearly orthogonal (ranging from 77.7°–88.2°) to their neighbors. The slight angular offset (2°–13°) created a rotational pattern that continued throughout the full thickness in fish and amphibians and to the very posterior layers in reptiles and birds. Interactions between lamellae were limited to “sutural” fibers in cartilaginous fish, and occasional lamellar branching in fish and amphibians. There was a marked increase in lamellar branching in higher vertebrates, such that birds ≫ reptiles > amphibians > fish. By contrast, mammalian corneas showed a nearly random collagen fiber organization with no orthogonal, chiral pattern.

CONCLUSIONS. Our data indicate that nonmammalian vertebrate corneas share a common orthogonal collagen structural organization that shows increased lamellar branching in higher vertebrate species. Importantly, mammalian corneas showed a different structural organization, suggesting a divergent evolutionary background.

Keywords: cornea, collagen, stroma, second-harmonic generation, nonlinear optical

Vision is our primary means of sensing our environment, and in the vertebrate eye visual acuity is dependent, in part, on the quality of the eye's refractive components, namely the lens and the cornea. The cornea specifically fulfills dual roles, acting as both a protective transparent cover that encases the inner parts of the eye, and as a refractive lens that focuses light back to the neurosensory retina. In its refractive role, the cornea's shape directly and significantly influences visual acuity, as evidenced by the success of refractive surgical procedures that are based largely on mechanical reshaping the anterior corneal surface. Although corneal shape is thought to be determined by the structure and biomechanics, the mechanisms regulating shape remain largely unknown.

Overall, the optical performance of the cornea is governed by the laws of refraction; specifically Snell's law, which dictates that when light impinges on a curved surface, the angle of refraction is proportional to the difference in refractive indices. The cornea, having a refractive index very close to that of water, is largely irrelevant in aquatic environments because it affects only a minor change in the angle of the incoming light rays when immersed in water regardless of the shape (Fig. 1).

On the other hand, when the cornea is surrounded by air, the difference in refractive indices is increased by several orders of magnitude, turning the cornea into a refractive element that can provide most of the eye's total refractive power depending on corneal curvature. For a refractive lens, control and maintenance of curvature or shape becomes an important functional requirement for the cornea. Because of its high refractive power, even comparatively minor deviations in corneal shape introduce optical aberrations that prevent the formation of a focused image on the retina, thereby reducing visual acuity. As shape is thought to be controlled by structure, one might expect that the transition from an aquatic to a terrestrial environment associated with the evolution of fish to tetrapods (Fig. 1) may be followed by structural changes important to the regulation of corneal shape and curvature. Although some extant species of fish have evolved both terrestrial and aquatic vision (e.g., *Anableps* and flying fish),^{1,2} and tetrapods have evolved aquatic species, a comparative structural analysis of the vertebrate cornea from different vertebrate clades may help elucidate clues to the structural evolution of the cornea to a refractive lens.

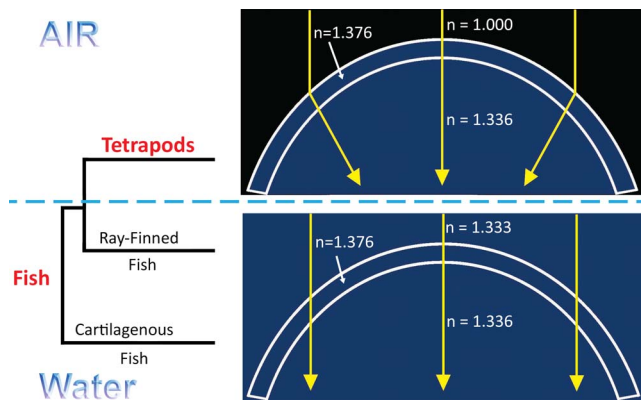


FIGURE 1. Different functional requirements for aquatic and terrestrial corneas. In a terrestrial environment (*top*), the difference in refractive indices between air and the cornea is large enough for the cornea to affect a significant change in direction of incoming light, making it a powerful refractive element. Under water, however (*bottom*), the cornea is essentially index-matched to the surrounding environment and therefore has very little refractive power.

We previously developed a second-harmonic generation (SHG)-based approach to three-dimensionally (3-D) reconstruct the collagen organization of the cornea at submicron resolution, called nonlinear optical high-resolution microscopy (NLO-HRMac).³ Using HRMac, we recently began to quantify the macrostructure of the mammalian cornea, and demonstrated a link between the degree of collagen lamellar branching and corneal compliance.⁴ Based on these findings, we proposed that collagen lamellar branching and anastomosing, in conjunction with transverse collagen lamellar orientation respective to the corneal surface,⁵ stabilizes corneal biomechanics and controls corneal shape in the mammalian cornea.^{5,6}

In this study, we tested the hypothesis that the evolution of a transparent cover to a refractive cornea involved structural changes in the collagen lamellar organization involving increased lamellar branching and anastomosis. Using HRMac, we show that corneas from cartilaginous and bony fish have a simple orthogonally arranged, rotational lamellar organization with little lamellar branching. By comparison, higher non-mammalian vertebrates, while also maintaining an orthogonal/

rotational organization, show increased lamellar branching that is greatest in birds, consistent with the hypothesis that increasing lamellar branching is associated with the evolution of a corneal refractive lens. Interestingly, the lamellar organization of the mammalian corneas is structurally unique from that of all other vertebrate clades, suggesting a previously unrecognized, evolutionary divergence.

METHODS

Vertebrate Eyes

Human and animal eyes were procured following institutional review board approval and in accordance with the tenets of the Declaration of Helsinki and the ARVO Statement for the Use of Animals in Ophthalmic and Vision Research. Marine mammal eyes (*Zalophus californianus*) were obtained from the California Marine Mammal Stranding Network with approval of the National Marine Fisheries Service. Human eyes were obtained from the San Diego Eye Bank. All procedures on laboratory animals were approved by the University of California-Irvine Institutional Animal Care and Use Committee. A list of all species and number of eyes evaluated in this study can be found in the Table.

Second-Harmonic Generation Imaging

Images were generated following previously established protocols for HRMac.^{3,4} Briefly, eyes were perfusion fixed under pressure with 2% paraformaldehyde in PBS (pH 7.4), corneas removed, and the tissue bisected and processed for en face SHG imaging or embedded in low melting point agarose (NuSieve GTG; Lonza, Rockland, ME, USA) for vibratome sectioning. Vibratome sections (250 μ m) were cut by using a Vibratome 1500 (Intracel, Ltd., Shepreth, UK).

En Face Tissue Imaging. For en face imaging, corneal tissue blocks taken from the central cornea ($\sim 3 \times 3$ mm) were placed epithelial side down on a POC-R environmental chamber (Carl Zeiss, Germany), overlaid with PBS, and through-focus images of SHG signals taken from the epithelial to endothelial surface at 2- μ m steps. Second-harmonic generation signals were generated using a $\times 40/1.2$ NA water immersion Zeiss Apochromat objective (Carl Zeiss) and a Zeiss LSM 510 Meta microscope (Carl Zeiss Imaging, Thornwood,

TABLE. List of Species Used for This Study

Species	Eyes, <i>n</i>	Clade	Elements	Rotation, deg	Separation, deg, Mean \pm SD
Great white shark (<i>Carcharodon carcharias</i>)	1	Chondrichthyes	Rotated sheets	220	82.6 \pm 5.5
Atlantic sharpnose shark (<i>Rhizoprionodon crenidens</i>)	2	Chondrichthyes	Rotated sheets	NA	NA
Sturgeon (<i>Acipenser transmontanus</i>)	2	Actinopterygii	Rotated sheets	247	85.9 \pm 2.4
Salmon (<i>Oncorhynchus gorboscha</i>)	2	Actinopterygii	Rotated sheets	135	77.7 \pm 6.3
Bullfrog (<i>Lithobates catesbeianus</i>)	4	Amphibia	Rotated sheets	119	82.3 \pm 4.3
Alligator (<i>Alligator mississippiensis</i>)	2	Reptilia	Rotated sheets	140	86.0 \pm 2.5
Chicken (<i>Gallus gallus</i>)	2	Aves	Rotated ribbons	175	88.2 \pm 1.3
Redtail Hawk (<i>Buteo jamaicensis</i>)	2	Aves	Rotated ribbons	NA	NA
Peregrine falcon (<i>Falco peregrinus</i>)	2	Aves	Rotated ribbons	213	86.2 \pm 2.8
Rabbit (<i>Oryctolagus cuniculus</i>)	4	Mammalia	Fiber bundles	NA	Random
Mouse (<i>Mus musculus</i>)	4	Mammalia	Fiber bundles	NA	Random
Sea lion (<i>Zalophus californianus</i>)	4	Mammalia	Fiber bundles	NA	Random
Dog (<i>Canis lupus familiaris</i>)	2	Mammalia	Fiber bundles	NA	Random
Human (<i>Homo sapiens</i>)	4	Mammalia	Fiber bundles	NA	Random

Rotated sheets are found in nonmammalian vertebrates up to bird corneas, which are made up of parallel intertwined ribbons. Both sheets and ribbons are layered nearly orthogonally. In birds and to a lesser degree in reptiles, the rotation ceases in the posterior cornea. Mammalian corneas consist of near-randomly oriented fiber bundles and do not exhibit a layered makeup.

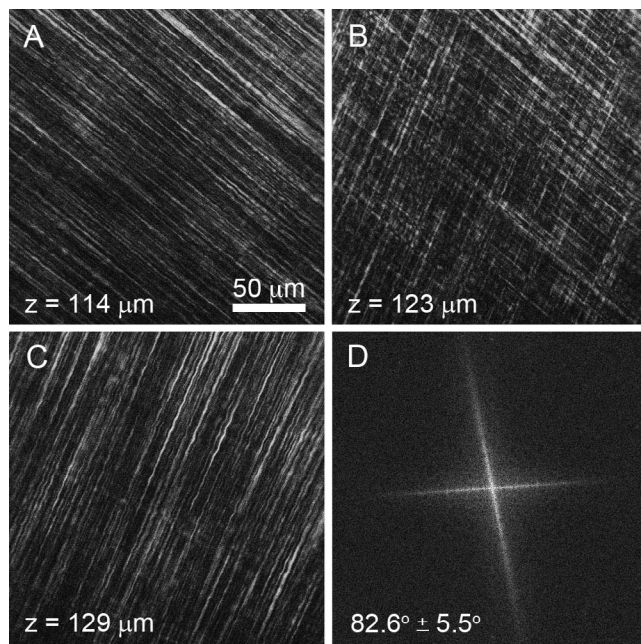


FIGURE 2. En face SHG images taken from great white shark cornea of two orthogonal lamellar planes (A, C) and the FFT analysis of the collagen orientation at the interface (B, D).

NY, USA) with a Chameleon femtosecond laser (Coherent, Inc., Santa Clara, CA, USA) tuned to 820 nm. To assess collagen rotation in the SHG through-focus data sets, 3-D Fast Fourier Transforms (FFTs) were generated by using custom-written software for ImageJ (<http://imagej.nih.gov/ij/>; provided in the public domain by the National Institutes of Health, Bethesda, MD, USA). Separation of lamellae was assessed by using the angle measurement tool in ImageJ, measuring and recording the acute angle between adjacent lamellae throughout the entire 3-D data set. The average and SD were then calculated and reported for the entire corneal stroma.

Vibratome Section Imaging. Transverse vibratome sections taken through the center of the cornea extending from limbus to limbus were placed in the POC-R environmental chamber and imaged using the Zeiss LSM 510 Meta and $\times 40/1.2$ NA objective. Second-harmonic generation signals were collected at 2- μm steps to a depth of 100 to 200 μm over the entire vibratome section. Individual 3-D image files were then digitally recombined to form large-scale, 3-D mosaics; 3-D renders were generated by using Amira software (Visage Imaging, Carlsbad, CA, USA). Fiber branching densities were determined by manually marking branching points in 3-D within a predefined volume by using Metamorph software (Molecular Devices, LLC, Sunnyvale, CA, USA).

RESULTS

Lamellar Orthogonality

En face, single-plane SHG images from the great white shark cornea are shown Figure 2. Each SHG image (Figs. 2A–C) represents a $225 \times 225\text{-}\mu\text{m}$ section of the anterior corneal stroma shown at a resolution of $0.44 \mu\text{m}/\text{pixel}$ taken at a stromal depth of 114 μm (Fig. 2A), 123 μm (Fig. 2B), and 129 μm (Fig. 2C) from the corneal epithelium. Through-focus SHG images showed alternating sheets of highly organized, parallel collagen fibers running in parallel and oriented nearly perpendicular or orthogonal to each other (Figs. 2A, 2C). At

the interface between collagen sheets, the orthogonal orientation of two adjacent sheets could be imaged (Fig. 2B) and an FFT generated showing the predominant directions of the collagen fibers in the two planes (Fig. 2D). The angular offset in fiber directionality between neighboring sheets measured by FFT analysis detected an average offset of $82.6^\circ \pm 5.5^\circ$ over the 3-D image data set for the great white shark. This pattern of nearly orthogonally arranged sheets of collagen fibers also was detected in other cartilaginous fish (sharpnose shark, not shown), bony fish (Fig. 3A1, salmon), and amphibians (Fig. 3B1, bullfrog). In reptiles (Fig. 3C1, alligator) and birds (Fig. 3D1, falcon), the collagen sheets appeared to be broken down into ribbons, but maintained an orthogonal orientation. Measurement of the angular offset (Figs. 3A2–D2) using FFT measurements also showed an average offset ranging from 77.7° to 88.2° for these different clades. As shown previously,⁷ SHG images taken from representative mammals (Figs. 3E1, 3E2, rabbit) showed lamellae to be organized into collagen ribbons having a random angle offset between lamellae in the same plane that was distinctly different from that of non-mammalian vertebrate corneas.

This offset from a truly orthogonal 90° angle introduced a clockwise, chiral-nematic pattern reminiscent of a cholesteric liquid crystal previously identified by Trelstad,⁸ resulting in a rotation of the collagen planes from the corneal epithelium through to the corneal endothelium. To better visualize these patterns, plane-by-plane FFTs were computed for each species, assembled as image stacks, and rendered in 3-D (Figs. 4A–F). Each spoke represents the predominant collagen orientation for a layer. The chiral pattern is present throughout the full stromal thickness in fishes (Fig. 4A, great white shark; Fig. 4B, salmon) and amphibians (Fig. 4C, bullfrog). However, in reptiles (Fig. 4D, alligator) and birds (Fig. 4E, falcon), the rotation of layers ceases in the posterior stroma, as the angular offset between adjacent layers changes to 90° . Note that the mammalian cornea (Fig. 4F, human) lacks any distinct spokes throughout the entire thickness of the stroma, indicating a random and not orthogonal arrangement between adjacent lamellae. To better compare these rotational patterns between species, an angular displacement of each layer as a function of corneal stromal depth was plotted (Fig. 4G). All nonmammalian vertebrate corneas evaluated showed similar angular displacement with depth, with some species showing more or less displacement due to the varying thickness of the collagen planes (compare great white shark with salmon). Overall, all nonmammalian species showed greater than 100° total angular displacement with both the great white shark and the falcon having more than 200° . Also note that the angular displacement of collagen planes stops in the posterior cornea for only the reptiles and birds (Fig. 4G, arrows).

Lamellar Branching

Because SHG signals from collagen fibers are dependent on the nonsymmetric orientation of the collagen molecules, SHG images detect only collagen fibers running parallel to the image plane. In nonmammalian corneas, such as the great white shark, this results in a banded SHG signal pattern in the stroma (Fig. 5). Each band can be related to the orientation of the collagen plane as detected by en face SHG imaging shown in the SHG image sequences from 1 to 16 above the transverse HRMac image shown in Figure 5. Starting at the far left, parallel collagen fiber orientation in the en face plane at images 1, 3, 12, and 14 can be associated with strong SHG bands noted at the corresponding arrows. Collagen fibers orthogonal to those planes show no SHG signal at images 2, 4, 13, and 15. A varying strength of SHG signal can be detected in collagen planes oriented between these in and out of plane positions as noted

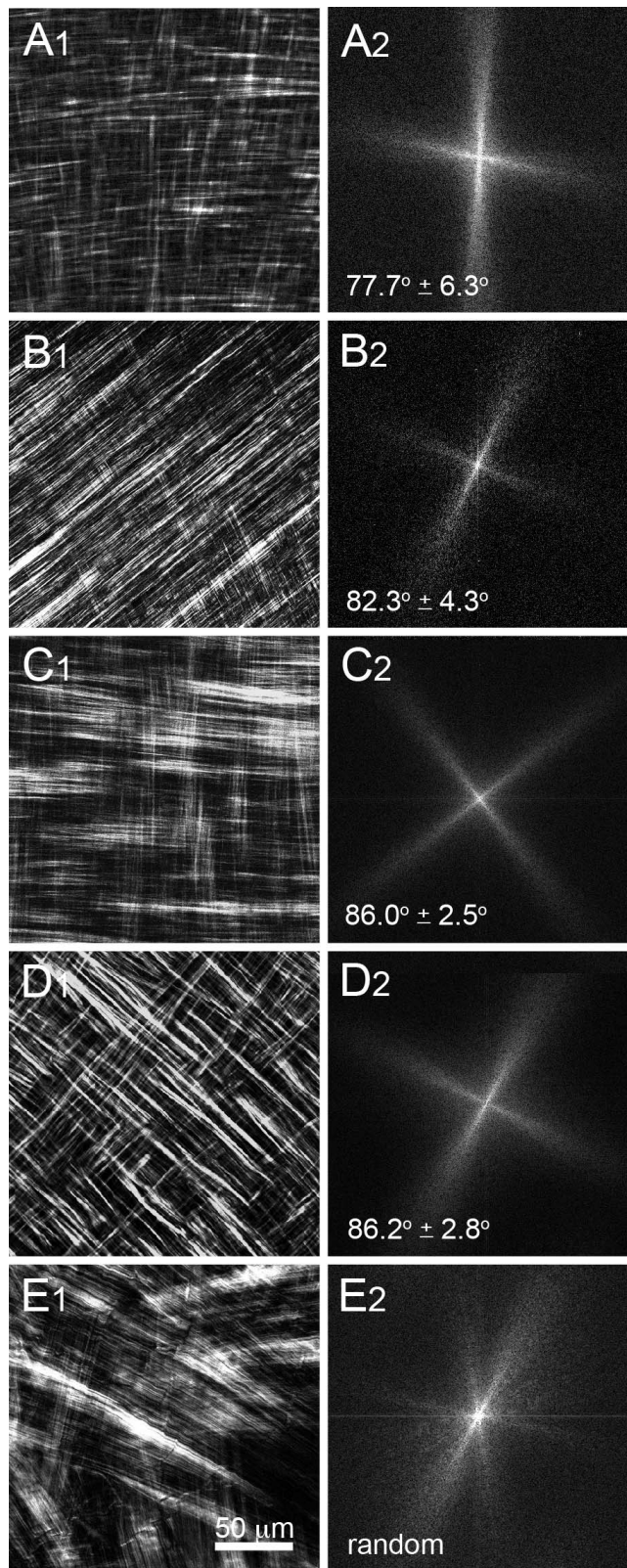


FIGURE 3. En face SHG images (1) and respective FFT analysis (2) of salmon (A), bullfrog (B), alligator (C), falcon (D), and rabbit (E). Collagenous orthogonal sheets were detected in salmon and bullfrog (A1, B1), whereas orthogonal lamellae formed ribbons in alligator (C1) and falcon (D1). Rabbit showed randomly oriented lamellar ribbons (E1). Orthogonal layers in nonmammalian vertebrate corneas were offset by 77.7° to 88.2°.

in images 5, 10, and 16. Overall, this reconstruction indicates that collagen fibers in a lamellar plane extend across the entire cornea from limbus to limbus, forming a sheet or cover that is as wide as it is long. This is shown more completely in Figure 6, where the corneal stroma of the falcon (Fig. 6A) and the Atlantic sharpnose shark (Fig. 6B) are reconstructed from limbus to limbus.

The NLO-HRM images of corneas from different species are shown in Figure 7. Corresponding high-resolution views can be found in Figure 8. Besides variations in corneal thickness between different species, the major difference was the presence of banding in nonmammalian vertebrate corneas, including great white shark, sturgeon, bullfrog, alligator, and falcon, which is absent in the mammalian human cornea. The close-up views in Figure 8 show the differences in corneal macrostructure between species. In fish, thick, straight collagen sheets run across the full width of the cornea. In the great white shark (Fig. 8A), this primary structural arrangement was supplemented by a secondary structure of thin, perpendicular “sutural” fibers (small arrows) previously noted by Payrau et al.⁹ Occasionally, collagen fibers could be identified that branched from one plane and extended down to a plane running in a parallel direction (Fig. 8A, large arrow). Beyond this comparatively rare branching detected in fish, there were no apparent links between collagen sheets.

The primary structural paradigm of rotating collagen sheets also was detected in bullfrog (Fig. 8C) and alligator (Fig. 8D) corneas; however, here the amount of branching and anastomosing was markedly increased. In the bird cornea (Fig. 8E), adjacent layers are highly interconnected by frequent branching and anastomosing, forming a structure that was reminiscent of chicken wire. Despite this increase in structural complexity, the underlying pattern is similar to that found in fish, amphibians, and reptiles: layers composed of many parallel collagen fibers, stacked nearly orthogonally in a chiral-nematic fashion.

Mammalian corneas (Fig. 8F) exhibited a radically different structural paradigm. Here, layered collagen sheets are replaced by more dynamic fiber bundles, which can be oriented in several different directions within the same plane and were no longer limited to individual planes or layers. Additionally, branching and anastomosing was not limited to the next nearest neighbors. Instead, fiber bundles often traversed many planes, especially in the anterior cornea, which was markedly more interwoven. The density of branching points for different clades is plotted in Figure 9. As suggested by the qualitative analysis of images from Figure 8, the density of branching points was lowest in fish, increased in amphibians, and was highest in birds. Mammalian data are not shown, as their corneas are based on a different structural paradigm, and as fiber-branching density changes markedly with stromal depth.

DISCUSSION

This study of the comparative structure of the vertebrate cornea points to three major findings. First, that collagen structural organization in all nonmammalian vertebrate corneas is built on an orthogonal/rotational or chiral-nematic paradigm reminiscent of cholesteric liquid crystals. Second, nonmammalian vertebrate corneas show increasing branching of collagen lamellae (sheets), such that fish < amphibian ≪ birds, consistent with the hypothesis that lamellar branching plays an important role in stabilizing corneal shape necessary for the development of a refractive lens. Third, that mammalian corneal structure, although having significant collagen fiber branching, shows a random pattern of adjacent lamellar

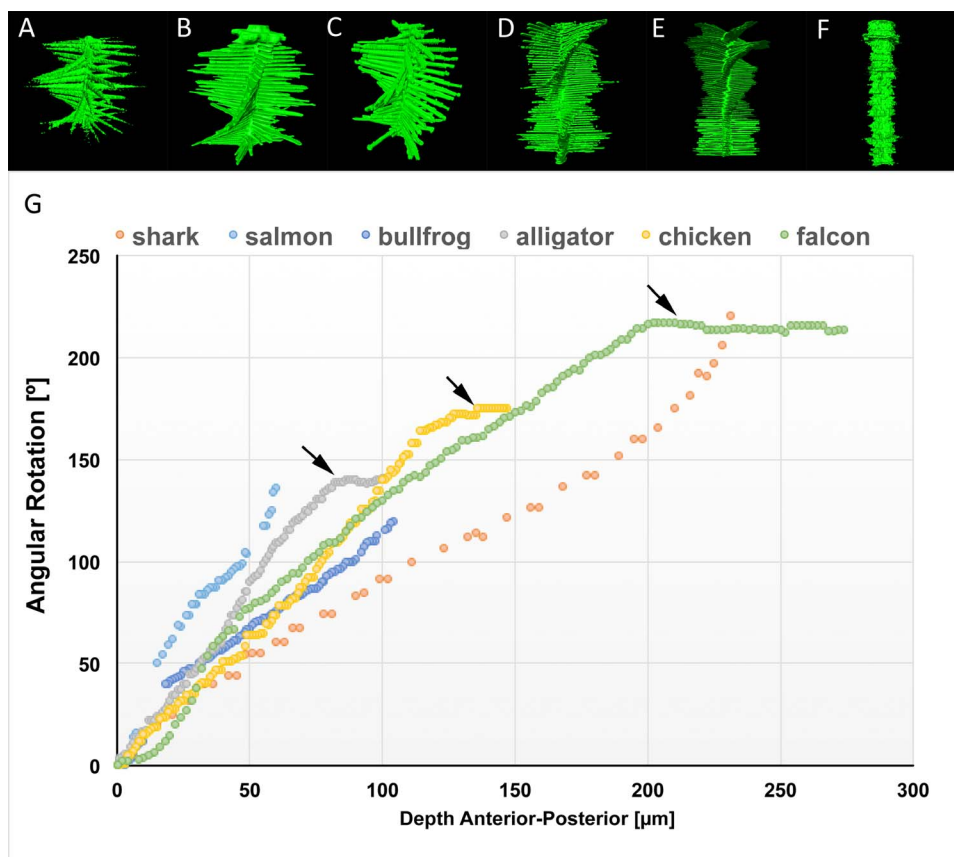


FIGURE 4. Three-dimensional FFTs of en face SHG stacks to highlight collagen fiber directionality in the great white shark (A), salmon (B), bullfrog (C), alligator (D), falcon (E), and human (F). Each spoke represents the predominant directionality of collagen fibers within each layer. A plot of the angular displacement with depth (G) for each species shows that nonmammalian vertebrate corneas rotate over 100° to 200°. Beginning with the alligator, the posterior layers are perpendicular, causing the rotation of adjacent layers to remain locked at fixed angles ([G], arrows).

organization that is divergent from other vertebrate corneas, suggesting a uniquely different developmental paradigm.

The orthogonal/rotational paradigm for corneal collagen structure was first identified by Trelstad and Coulombre in 1971.¹⁰ In this detailed study of serially sectioned, silver-stained, staged chick embryonic corneas, these investigators showed that the primary stroma deposited by the corneal epithelium was first laid down in a rotational pattern before mesenchymal invasion and secondary stromal deposition. This pattern was unique in that the first lamellae deposited composed of a single layer of collagen fibrils was completely

orthogonal showing no rotation, whereas later lamellae deposited by the epithelium showed a consistent clockwise, rotational deposition. Because adult corneas maintained this same rotational pattern, albeit with thicker lamellae and bundled fibrils, Trelstad and Coulombre¹⁰ proposed that the primary stroma laid down by the epithelium formed a template for the deposition of secondary stroma by the invading mesenchyme. One explanation for this depositional pattern posited by the authors was a self-assembly system in which the matrix guided the development of structure; a hypothesis supported by the finding that a clockwise rotational pattern

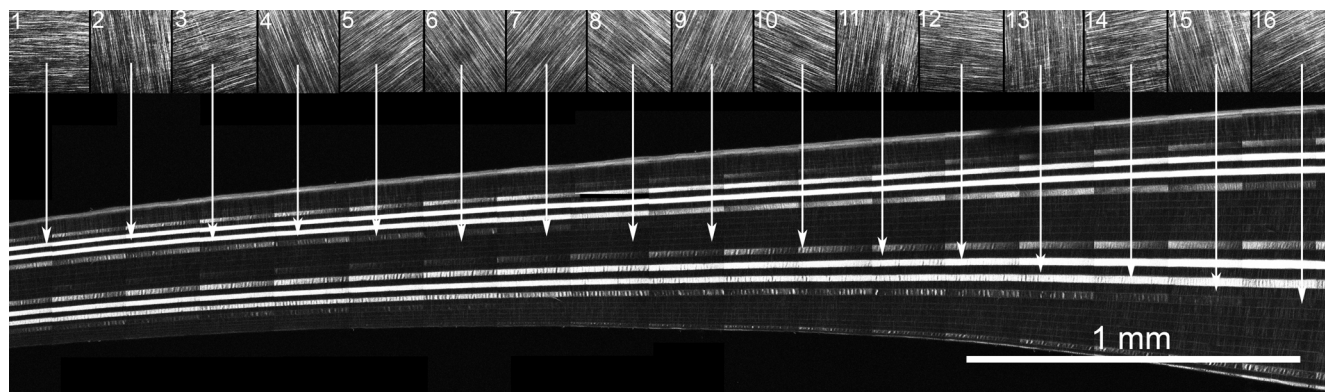


FIGURE 5. Cross-sectional HRMac image of great white shark cornea showing the plywood-like organizational pattern and the representative directionality of the collagen lamellae at each band (1-16, arrows).

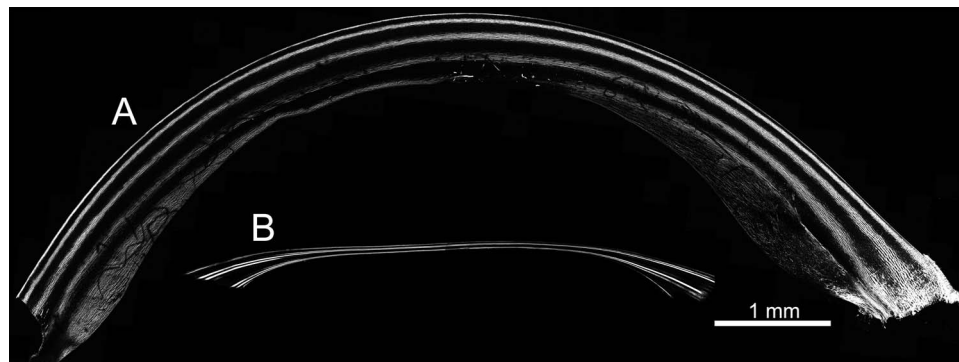


FIGURE 6. Cross-sectional HRMac image of the falcon (A) and the Atlantic sharpnose shark (B).

was found in both left and right eyes, indicating a bilateral asymmetrical architecture about the midline of the developing embryo. Later studies also established that lower vertebrates, including frog, turtle, and carp, had similar angular displacement of lamellae reminiscent of cholesteric liquid crystal, further supporting a self-assembly model for the organization of the corneal stroma.⁸

The findings presented in this study by using nonlinear optical imaging of SHG signals from collagen are consistent with those of Trelstad and Coulombre¹⁰ and show for the first time that the angular displacement between adjacent collagen lamellae is conserved, ranging from 88.2° to 77.7° in a series of nonmammalian corneas from different clades. This limited range further supports a self-assembly system as proposed, where interactions between collagen fibrils guide the orientation and direction of adjacent fibrils. Although Trelstad and Coulombre¹⁰ recognized that the spatial separation between fibrils may preclude a direct interaction, indirect interactions mediated by bridging matrix components, such as glycosaminoglycan, may participate in this process. Our findings that lower vertebrate clades, including cartilaginous and boney fish, have the same angular displacement as birds also suggest that these potential “bridging” molecules are conserved in the nonmammalian vertebrate cornea. However, it should be noted that these “orientation” cues and bridging molecules need to be localized to the interface between lamellae and not specific to collagen fibrils; otherwise, bundling of fibrils to form thicker lamellae and fiber bundles could not be accomplished.

Another finding in our study that was not shown by earlier work is that individual collagen lamellae extend in a uniform sheet that covers the cornea from limbus to limbus in nonmammalian eyes. This is most strikingly shown in the HRMac images of fish, in which the same lamellae can be traced, uninterrupted, from one side of the cornea to the other. Although SHG signals do not detect individual collagen fibrils, it seems likely that fibrils extend over millimeters to centimeters in the cornea. Furthermore, the banded pattern shown by the SHG HRMac due to the angular displacement of the collagen fibers suggests clear structural similarities to plywood. Because alternating thin veneers of wood bonded together are stronger to bending stresses than a single thick piece, it would seem that nature has adopted a similar structural design in the construction of the nonmammalian vertebrate cornea. Although we are evaluating only extant species and there is no paleontological record for corneal structure, one might propose that this simple, plywood design may represent the earliest structure of the cornea to form a cover for the vertebrate camera eye.

Our second finding was that higher nonmammalian vertebrate corneas showed greater collagen lamellar branching, such that birds \gg reptiles $>$ amphibians $>$ fish.

Rudimentary lamellar branching was detected in both cartilaginous and boney fish, although the most noted feature in fish was the presence of “sutural” fibers detected in Elasmobranchs. “Sutural” fibers were first described by Ranvier in 1878,¹¹ and their effects on swelling and transparency in the Elasmobranch cornea have been studied by various investigators.^{9,12,13} Many species of Elasmobranchs have been reported to lack a corneal endothelium, and the presence of these ‘sutural’ fibers has been suggested to represent the underlying structural adaptation responsible for the resistance to corneal swelling and the maintenance of transparency in these species. It should be noted that the lamprey, which is ancestral to fish, also have ‘sutural’ fibers and lack a corneal endothelium,¹⁴ supporting the hypothesis that the structure of the ancestral cornea assumed a plywood-like design held rigidly together by ‘sutural’ fibers.

Developmental studies in skates indicate that cartilaginous fish undergo a very similar developmental program to that of birds, in which the primary stroma deposited by the corneal epithelium forms a template for the deposition of the secondary stroma by the invading mesenchyme.¹² Although “sutural” fibers are not detected in adult corneas of higher vertebrates with a functional corneal endothelium, transverse collagen fibers extending from the corneal epithelium perpendicular into the stroma have been noted in the developing avian cornea by Hay and Revel.¹⁵ These findings support the old axiom that ontogeny recapitulates phylogeny, suggesting that “sutural” fibers in the developing avian stroma are vestigial and their function potentially replaced by collagen lamellar branching. In this regard, an interesting difference between fish and amphibians and reptiles and birds is that the primary stroma undergoes an organizational change from sheets or plies to ribbons or belts, a finding also noted by Trelstad and Coulombre.¹⁰ The breakdown of collagen sheets to ribbons would have the obvious developmental advantage of facilitating assembly of an interwoven stroma with 3-D branching and anastomosing of collagen lamellae. Although the evolutionary driving forces for these structural changes are not known, they are consistent with our hypothesis that collagen branching and regional stiffening of the corneal stroma plays an important role in regulating corneal shape and, consequently, the design of a corneal refractive lens.

Although the developmental program controlling lamellar weaving is not known, studies by Trelstad and Coulombre¹⁰ indicate that the primary stroma may be laid down in a sinusoidal pattern, which if similar to the chicken-wire pattern identified by HRMac would again support the view that the lamellae may self-assemble into a branching and anastomosing pattern. Other developmental studies, particularly in tendon, indicate that collagen fibril assembly may be directed within specialized extracellular compartments or fibroblast “fibropo-

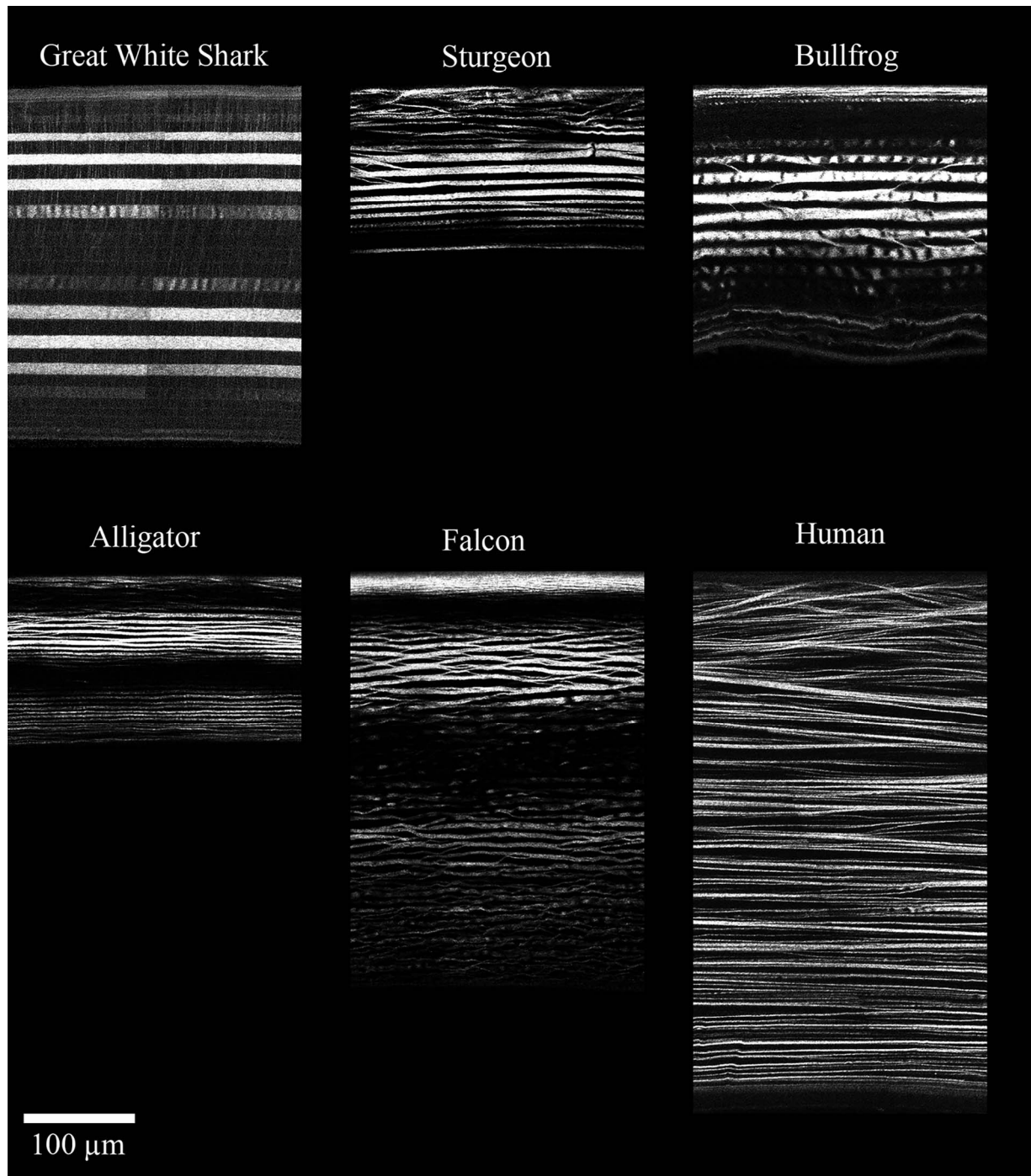


FIGURE 7. Full-thickness, cross-sectional HRMac images of different vertebrate corneas.

sitors.”¹⁶ Similar structures also have been identified in the developing avian cornea using high-voltage electron microscopy and more recently by volume scanning electron microscopy.^{17,18} Needless to say, the cellular, molecular, and mechanical events that orchestrate the collagen fibril bundling, branching, and anastomosing that is evident in higher vertebrates remains a mystery and needs further study.

Our final finding in this comparative structural study was that mammalian stromal organization was characterized by a radically different structural paradigm from that of other vertebrate corneas. Although like reptiles and birds, mammalian corneal lamellae are organized into ribbons, there is a loss

of the orthogonal/rotational organization between adjacent lamellae, giving a random organizational pattern. This finding is in agreement with Polack,¹⁹ who noted that silver-stained collagen fibers crossed each other only occasionally at right angles, unlike collagen fiber organization in lower vertebrates. From a mechanical standpoint, this structural change may have two important implications. First, the orthogonal orientation of lamellae results in differential distribution of strain with greatest resistance parallel to the axis of the lamellae. To achieve an even 360° distribution of strain over the entire stroma, alternate collagen lamellae must rotate at least over 90°. In the mammalian stroma, multiple lamellae within a

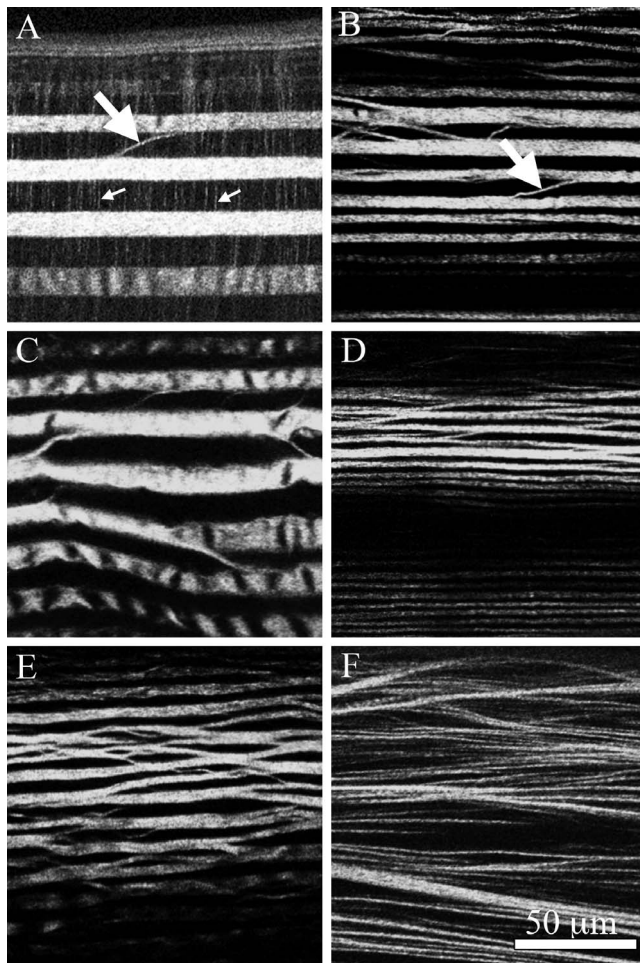


FIGURE 8. Corresponding high-resolution HRMac views of vertebrate corneas. The shark cornea (A) shows thick, straight bands of collagen lamellae interconnected by “sutural” fibers (*small arrows*) and occasional lamellar branching (*large arrow*) and anastomosis. The sturgeon cornea (B) is similarly structured but appears to lack the perpendicular sutural fibers. Fiber branching is more frequent in the bullfrog cornea (C), and even more prominent in the alligator cornea (D). The bird cornea (E) has the highest amount of branching and anastomosis of all nonmammalian corneas, but appears to be based on the same underlying structure. Human corneas (F), however, show a completely different structural paradigm, abandoning layers in favor of highly interconnected fiber bundles and transverse fibers that are most pronounced in the anterior cornea.

single plane oriented at different angles results in a more uniform distribution of stain, and a more stable structure compared with the orthogonal arrangement. Second, in an orthogonal arrangement, collagen fibers are restrained within a single plane, limiting their interactions or branching to adjacent lamellae immediately above or below. By comparison, randomly arranged fibers are not constrained within a single plane and can traverse anteriorly or posteriorly to connect to lamellae at much greater axial distances. This would provide for complete interconnection of lamellae leading to a self-stabilizing structure that is not dependent on an orthogonal/rotational pattern.

The cause of this divergent structural organization is not known; however, as part of the outer tunic of the eye, the cornea interfaces with the sclera at the limbus, which represents a boundary condition for the system of corneal biomechanics. Mammals lack the bony ossicle at the corneal-scleral interface that is found in birds,²⁰ reptiles,²¹ and fish.²² It

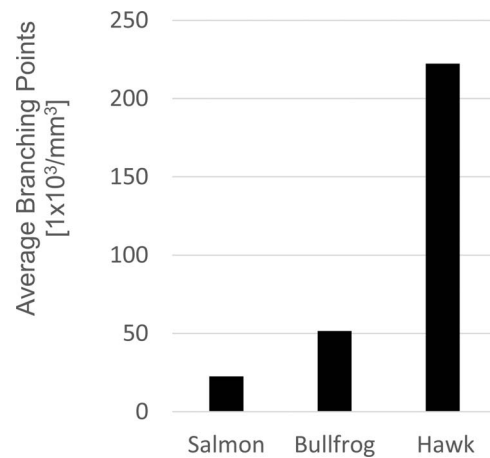


FIGURE 9. Volume density of fiber branching points by species. Fiber points were counted manually in a predefined volume. Branching is rare in sharks and other fish. The density of branching points increases in amphibians. The highest density of fiber branching is found in birds and mammals.

is conceivable that the differences in corneal structure between mammals and other vertebrates is also linked to these differing boundary conditions. The presence of a comparatively rigid scleral ossicle provides stabilization for the cornea and represents a natural boundary that allows for differentiation of curvature between cornea and sclera. Mammalian corneas, which lack this scleral ossicle, need to be self-stabilizing, which is presumably achieved through the random ribbon lamellar organization and the presence of collagen lamellae that interconnect anterior and posterior collagen fibers.^{4,5}

Another major difference between mammals and other vertebrates is that the development of the corneal stroma does not require the deposition of an acellular primary stroma. In chick and Elasmobranchs, the primary stroma that is organized by the corneal epithelium is thought to direct the alignment of the secondary stroma deposited by the invading fibroblasts.^{12,15} As identified by Haustein,²³ the developing mouse cornea lacks a primary stroma, and hence topographical cues are not present during collagen deposition by the invading mammalian keratocytes. Although this may help explain the random organization, what cues direct collagen fiber organization and control corneal shape are unknown. Although our studies indicate that adjacent lamellar organization is random, work by Meek and Boote²⁴ using X-ray scattering has shown that there is a preferential orientation of collagen along the major superior-inferior and nasal-temporal meridian. As suggested by the authors, these findings indicate that mechanical forces may provide cues for alignment of collagen. Similar regional and more local mechanical cueing also may be involved in directing corneal morphogenesis in mammals.

In summary, this comparative study of the vertebrate corneal stromal structure has identified distinct differences in the organization of collagen lamellae between different vertebrate clades. In fish, the corneal stroma has an organizational structure similar to that of plywood, with collagen lamellae organized as sheets or plies in a distinct orthogonal/rotational pattern. Although variations in structure were noted, it is likely that the plywood structure is an ancestral paradigm producing a flat corneal cover, on which structural adaptations such as lamellar branching and anastomoses evolved to stiffen the cornea, reduce shear stress, and ultimately alter or control corneal shape in higher vertebrates. In mammals, this orthogonal/rotational paradigm is lost and replaced with a

random lamellar pattern that is a divergent developmental paradigm compared with the other vertebrate corneas evaluated. We postulate that this structural change provides for a more uniform distribution of stresses and strains within the corneal stroma and facilitates the development of a self-stabilizing stromal structure. However, the cellular, molecular, and mechanical mechanisms controlling the bundling, branching, and anastomosing of collagen remain unknown.

Acknowledgments

Supported in part by National Eye Institute Grant EY018665.

Disclosure: **M. Winkler**, None; **G. Shoa**, None; **S.T. Tran**, None; **Y. Xie**, None; **S. Thomasy**, None; **V.K. Raghunathan**, None; **C. Murphy**, None; **D.J. Brown**, None; **J.V. Jester**, None

References

- Swamynathan SK, Crawford MA, Robison WG Jr, Kanungo J, Piatigorsky J. Adaptive differences in the structure and macromolecular compositions of the air and water corneas of the "four-eyed" fish (*Anableps anableps*). *FASEB J*. 2003;7:1996-2005.
- Baylor ER. Air and water vision of the Atlantic flying fish, *Cypselurus heterurus*. *Nature*. 1967;214:307-309.
- Jester JV, Winkler M, Jester BE, Nien C, Chai D, Brown DJ. Evaluating corneal collagen organization using high resolution non linear optical (NLO) macroscopy. *Eye Contact Lens*. 2010;36:260-264.
- Winkler M, Chai D, Kriling S, et al. Nonlinear optical macroscopic assessment of 3-D corneal collagen organization and axial biomechanics. *Invest Ophthalmol Vis Sci*. 2011;52:8818-8827.
- Winkler M, Shoa G, Xie Y, et al. Three-dimensional distribution of transverse collagen fibers in the anterior human corneal stroma. *Invest Ophthalmol Vis Sci*. 2013;54:7293-7301.
- Thomasy SM, Raghunathan VK, Winkler M, et al. Elastic modulus and collagen organization of the rabbit cornea: epithelium to endothelium. *Acta Biomater*. 2014;10:785-791.
- Morishige N, Petroll WM, Nishida T, Kenney MC, Jester JV. Noninvasive corneal stromal collagen imaging using two-photon-generated second-harmonic signals. *J Cataract Refract Surg*. 2006;32:1784-1791.
- Trelstad RL. The bilaterally asymmetrical architecture of the submammalian corneal stroma resembles a cholesteric liquid crystal. *Dev Biol*. 1982;92:133-134.
- Payrau P, Pouliquen Y, Faure MP, Offret G. Ultrastructure des fibres suturales de la cornee des poissons Elasmobranches. *Arch Ophthalmol (Paris)*. 1965;25:745-754.
- Trelstad RL, Coulombre AJ. Morphogenesis of the collagenous stroma in the chick cornea. *J Cell Biol*. 1971;50:840-858.
- Ranvie L. *Lecons d'Anatomie Generale Faites au College de France, 9th Lecon, la Cornee*. Librairie J.B. Baillere et fils: Paris; 1878.
- Conrad GW, Paulsen AQ, Luer CA. Embryonic development of the cornea in the eye of the clearnose skate, *Raja eglanteria*: I. Stromal development in the absence of an endothelium. *J Exp Zool*. 1994;269:263-276.
- Goldman JN, Benedek GB. The relationship between morphology and transparency in the nonswelling corneal stroma of the shark. *Invest Ophthalmol Vis Sci*. 1967;6:574-600.
- Van Horn DL, Edelhauser HF, Schultz RO. Ultrastructure of the primary spectacle and cornea of the sea lamprey. *J Ultrastruct Res*. 1969;26:454-464.
- Hay ED, Revel JP. *Fine Structure of the Developing Avian Cornea*. Vol. 1. S. Karger: New York; 1969.
- Birk DE, Trelstad RL. Extracellular compartments in tendon morphogenesis: collagen fibril, bundle, and macroaggregate formation. *J Cell Biol*. 1986;103:231-240.
- Birk DE, Trelstad RL. Extracellular compartments in matrix morphogenesis: collagen fibril, bundle, and lamellar formation by corneal fibroblasts. *J Cell Biol*. 1984;99:2024-2033.
- Young RD, Knupp C, Pinali C, et al. Three-dimensional aspects of matrix assembly by cells in the developing cornea. *Proc Natl Acad Sci U S A*. 2014;111:687-692.
- Polack FM. Morphology of the cornea. I. Study with silver stains. *Am J Ophthalmol*. 1961;51:1051-1056.
- Coulombre A, Coulombre J, Mehta H. The skeleton of the eye: I. Conjunctival papillae and scleral ossicles. *Dev Biol*. 1962;5:382-401.
- Lee LP, Szema R. Inspirations from biological optics for advanced photonic systems. *Science*. 2005;310:1148-1150.
- Mullaney J, Coffey V, Fenton M. Atavistic ocular ossicle. *Br J Ophthalmol*. 1971;55:243.
- Haustein J. On the ultrastructure of the developing and adult mouse corneal stroma. *Anat Embryol (Berl)*. 1983;168:291-305.
- Meek KM, Boote C. The use of X-ray scattering techniques to quantify the orientation and distribution of collagen in the corneal stroma. *Prog Retin Eye Res*. 2009;28:369-392.